



Citation for published version:

Deng, Y, Eames, C, Chotard, JN, Laleire, F, Seznec, V, Emge, S, Pecher, O, Grey, CP, Masquelier, C & Islam, MS 2015, 'Structural and mechanistic insights into fast lithium-ion conduction in $\text{Li}_3\text{SiO}_4\text{-Li}_3\text{PO}_4$ solid electrolytes', *Journal of the American Chemical Society*, vol. 137, no. 28, pp. 9136-9145.
<https://doi.org/10.1021/jacs.5b04444>

DOI:

[10.1021/jacs.5b04444](https://doi.org/10.1021/jacs.5b04444)

Publication date:

2015

Document Version

Peer reviewed version

[Link to publication](#)

This document is supplementary material supplied with the Accepted Manuscript version of a Published Work that appeared in final form in *Journal of the American Chemical Society*, copyright © American Chemical Society after peer review and technical editing by the publisher. To access the final edited and published work see <http://pubs.acs.org/doi/abs/10.1021/jacs.5b04444>

University of Bath

Alternative formats

If you require this document in an alternative format, please contact:
openaccess@bath.ac.uk

General rights

Copyright and moral rights for the publications made accessible in the public portal are retained by the authors and/or other copyright owners and it is a condition of accessing publications that users recognise and abide by the legal requirements associated with these rights.

Take down policy

If you believe that this document breaches copyright please contact us providing details, and we will remove access to the work immediately and investigate your claim.

Structural and mechanistic insights into fast lithium-ion conduction in $\text{Li}_4\text{SiO}_4\text{-Li}_3\text{PO}_4$ solid electrolytes

Yue Deng^{†‡}, Christopher Eames[‡], Jean-Noël Chotard[†], Fabien Lalère[†], Vincent Seznec[†], Steffen Emge[§], Oliver Pecher[§], Clare P. Grey[§], Christian Masquelier[†], M. Saiful Islam^{†*}

[†] Laboratoire de Réactivité et Chimie des Solides (UMR CNRS 7314), Université de Picardie Jules Verne, 33 rue Saint Leu, 80039 Amiens Cedex, France

[‡] Department of Chemistry, University of Bath, Bath, BA2 7AY, UK

[§] Department of Chemistry, University of Cambridge, Cambridge, CB2 1EW, UK

Supplementary Information

Table S1. Experimental data for the Li₄SiO₄ single crystal x-ray diffraction measurements

Crystal data	
Chemical formula	Li ₄ SiO ₄
M_r	119.85
Crystal system, space group	Monoclinic, $P2_1/m$
a, b, c (Å)	11.5556(4), 6.0986(2), 16.7300(5)
β (°)	99.058(1)
V (Å ³), V/Z (Å ³)	1164.31(7), 83.16(2)
Z	14
Dx (kg m ⁻³)	2.393 x 10 ³
μ (mm ⁻¹) for Mo K α , $\lambda = 0.71073$ Å	0.54
Crystal size (mm)	0.13 x 0.15 x 0.19
Data collection	
Diffractometer	Bruker D8 Venture APEXII
Temperature	293K
Scan mode	ϕ and ω scan
θ min-max (°)	2.3 - 49.2
R(int) (%)	2.8
Recording reciprocal space	$h = -24 \rightarrow 24, k = -12 \rightarrow 11, l = -35 \rightarrow 26$
Refinement	
Independent reflections	12402
Reflections with $I > 2\sigma(I)$	7938
No. refined parameters	331
Refine method	F ²
R[F ² > 2 σ (F ²)]	0.041
wR(F ²)	0.149
S	0.90
$\Delta\rho_{\max}/\Delta\rho_{\min}$ (e Å ⁻³)	1.20 / -1.19

Table S2. BPP fit parameters for the ${}^7\text{Li}$ VT (320 – 875 K) T_1 data based on the $\frac{1}{T_1} = C \left(\frac{\tau_c}{1+\omega_0^2\tau_c^2} + \frac{4\tau_c}{1+4\omega_0^2\tau_c^2} \right) + A \cdot T^2 - B$ functional with $\tau_c = \tau_0 \cdot e^{E_a/RT}$. Single standard deviations are given in parenthesis.

Sample	$C / 10^9 \text{ s}^{-2}$	$A / 10^{-5} \text{ s}^{-1}\text{K}^{-2}$	B / s^{-1}	$\tau_0 / 10^{-11} \text{ s}$	E_a / eV
$\text{Li}_{3.25}\text{Si}_{0.25}\text{P}_{0.75}\text{O}_4$	12.0(5)	-9.1(1)	-1.0 (1)	1.20(1)	0.21(2)
$\text{Li}_{3.5}\text{Si}_{0.5}\text{P}_{0.5}\text{O}_4$	10.0(5)	-5.6(1)	-0.8(1)	0.63(1)	0.23(2)
$\text{Li}_{3.75}\text{Si}_{0.75}\text{P}_{0.25}\text{O}_4$	8.5(5)	-1.3(1)	-0.9(1)	3.40(2)	0.18(3)

Table S3. Interatomic potential parameters used for structural modeling and energy minimization calculations. The potentials are described by the equation: $U(r) = \frac{z_i z_j e^2}{r} + D_{ij} \left[\left\{ 1 - e^{-a_{ij} \times (r-r_0)} \right\}^2 - 1 \right] + \frac{C_{ij}}{r^{12}}$

	D_{ij} (eV)	a_{ij} (\AA^{-2})	r_0 (\AA)	C_{ij} (eV \AA^{12})
$\text{Li}^{0.6}\text{---O}^{-1.2}$	0.001115	3.4294	2.68136	1.0
$\text{Si}^{2.4}\text{---O}^{-1.2}$	0.340554	2.0067	2.10000	1.0
$\text{P}^{3.0}\text{---O}^{-1.2}$	0.831326	2.5858	1.80079	1.0
$\text{O}^{-1.2}\text{---O}^{-1.2}$	0.042395	1.3793	3.61870	22.0

Table S4. Crystallographic data of $\text{Li}_{3.5}\text{Si}_{0.5}\text{P}_{0.5}\text{O}_4$ derived from Rietveld refinements of room temperature powder neutron diffraction patterns and selected interatomic distances (Å) and angles (°). For the Si/PO_4 (or LiO_n) polyhedra, the italicized numbers on the diagonal represent the Si/P-O (or Li-O) distances, the numbers above the diagonal are O-Si/P-O (or O-Li-O) angles and the numbers below the diagonal are O-O distances.

$\text{Li}_{3.5}\text{Si}_{0.5}\text{P}_{0.5}\text{O}_4$		
S.G.: <i>Pnma</i> ;	$Z = 4$	
$a = 10.5892(2)\text{Å}$	$b = 6.1152(2)\text{Å}$	$c = 5.0056(2)\text{Å}$
$V = 324.137(5)\text{Å}^3$	$V/Z = 81.034\text{Å}^3$	$\sum \text{Occ.}(\text{Li}) = 3.30(14) / \text{f.u.}$
$R_{\text{wp}} = 12.9\%$	$R_{\text{bragg}} = 4.92\%$	$\chi^2 = 3.88$

Atomic position							
atom	Wyckoff position	x/a	y/b	z/c	occupancy	Biso	BVS
Li1	8 <i>d</i>	0.1626(10)	0.0032(11)	0.1891(14)	0.781(16)	0.93(12)	1.058(13)
Li2	4 <i>c</i>	0.4293(13)	1/4	0.3174(18)	0.80(2)	0.93(12)	0.989(14)
Li3	4 <i>c</i>	0.382(5)	1/4	0.129(12)	0.156(18)	0.93(12)	0.81(5)
Li4	8 <i>d</i>	0.018(5)	0.051(8)	0.055(9)	0.119(11)	0.93(12)	1.02(7)
Li5	8 <i>d</i>	0.153(4)	0.536(5)	0.368(6)	0.200(14)	0.93(12)	1.08(6)
Li6	4 <i>c</i>	0.289(6)	1/4	0.015(11)	0.144(16)	0.93(12)	0.61(4)
Si/P	4 <i>c</i>	0.0888(4)	1/4	0.6750(6)	0.5/0.5	0.71*	4.42/4.33(2)
O1	8 <i>d</i>	0.3405(2)	0.5382(3)	0.2799(4)	1	0.95*	1.849(13)
O2	4 <i>c</i>	0.4472(2)	1/4	0.7193(5)	1	0.63*	1.990(18)
O3	4 <i>c</i>	0.0895(3)	1/4	0.3577(5)	1	0.95*	2.021(17)

*Anisotropic thermal parameters (Å²) x 10⁻⁴						
	B11	B22	B33	B12	B13	B23
Si/P	16(3)	37(10)	73(14)	0	3(7)	0
O1	16(2)	76(5)	99(8)	0(3)	2(3)	-11(6)
O2	11(3)	32(7)	100(13)	0	-9(5)	0
O3	21(3)	71(9)	89(12)	0	7(6)	0

Si/PO₄	O1^{a**}	O1^b	O2	O3
O1 ^a	<i>1.585(3)</i>	109.6(2)	109.6(3)	109.2(2)
O1 ^b	2.590(3)	<i>1.585(3)</i>	109.6(3)	109.2(2)
O2	2.594(3)	2.594(3)	<i>1.590(5)</i>	109.7(3)
O3	2.587(3)	2.587(3)	2.599(4)	<i>1.588(4)</i>

Table S4 (continued)

Li(1)O₄	O1 ^a	O1 ^b	O2	O3
O1 ^a	2.060(7)	105.1(4)	98.7(3)	110.7(3)
O1 ^b	3.187(3)	1.954(11)	117.1(4)	113.2(4)
O2	3.037(3)	3.324(3)	1.942(8)	110.8(3)
O3	3.255(3)	3.213(3)	3.1591(9)	1.895(8)

Li(2)O₄	O1 ^a	O1 ^b	O2	O3
O1 ^a	2.006(7)	123.0(3)	97.9(4)	111.9(5)
O1 ^b	3.525(3)	2.006(7)	97.9(4)	111.9(5)
O2	3.037(3)	3.037(3)	2.021(9)	111.9(5)
O3	3.245(3)	3.245(3)	3.258(4)	1.910(13)

Li(3)O₄	O1 ^a	O1 ^b	O2	O3
O1 ^a	1.97(3)	127.3(11)	115.8(18)	102.2(16)
O1 ^b	3.525(3)	1.97(3)	115.8(18)	102.2(16)
O2	3.501(3)	3.501(3)	2.16(6)	73(2)
O3	3.245(3)	3.245(3)	2.599(4)	2.20(5)

Li(4)O₅	O1 ^a	O1 ^b	O2 ^a	O2 ^b	O3
O1 ^a	2.12(5)	154(2)	95(2)	77.0(19)	100.8(19)
O1 ^b	4.060(3)	2.04(5)	80(2)	96.2(19)	104.2(19)
O2 ^a	3.037(3)	2.594(3)	1.99(5)	154.0(19)	106.1(19)
O2 ^b	2.594(3)	3.037(3)	3.927(2)	2.04(5)	99.7(19)
O3	3.245(3)	3.255(3)	3.258(4)	3.1591(9)	2.09(5)

Li(5)O₄	O1 ^a	O1 ^b	O2	O3
O1 ^a	2.04(4)	100.1(14)	117.8(16)	110.2(15)
O1 ^b	3.187(3)	2.11(3)	124.8(14)	80.8(13)
O2	3.324(3)	3.501(3)	1.84(3)	116.9(15)
O3	3.213(3)	2.587(3)	3.1591(9)	1.87(3)

Li(6)O₅	O1 ^a	O1 ^b	O1 ^c	O1 ^d	O2
O1 ^a	2.22(5)	71.3(18)	90.3(16)	155.4(16)	96(2)
O1 ^b	2.590(3)	2.22(5)	155.4(16)	90.3(16)	96(2)
O1 ^c	3.187(3)	4.392(3)	2.27(4)	101.7(13)	101.9(18)
O1 ^d	4.392(3)	3.187(3)	3.525(3)	2.27(4)	101.9(18)
O2	3.324(3)	3.324(3)	3.501(3)	3.501(3)	2.24(6)

**O1^a (x, y, z), O1^b (x, 1/2-y, z), O1^c (1/2-x, -y, 1/2+z), O1^d (1/2-x, y-1/2, 1/2+z); O2^a (x, y, z), O2^b (-x, -y, -z)

Table S5. Crystallographic data of $\text{Li}_{3.75}\text{Si}_{0.75}\text{P}_{0.25}\text{O}_4$ derived from Rietveld refinements of room temperature powder neutron diffraction patterns and selected interatomic distances (Å) and angles (°). For the Si/PO_4 (or LiO_n) polyhedra, the italicized numbers on the diagonal represent the Si/P-O (or Li-O) distances, the numbers above the diagonal are O-Si/P-O (or O-Li-O) angles and the numbers below the diagonal are O-O distances.

$\text{Li}_{3.75}\text{Si}_{0.75}\text{P}_{0.25}\text{O}_4$			
S.G.: $P2_1/m$;	$Z = 2$		
$a = 5.1054(2)\text{Å}$	$b = 6.1123(2)\text{Å}$	$c = 5.2967(2)\text{Å}$	$\beta = 90.370(2)^\circ$
$V = 165.281(6)\text{Å}^3$	$V/Z = 82.640\text{Å}^3$	$\sum \text{Occ.}(\text{Li}) = 3.61(14) / \text{f.u.}$	
$R_{\text{wp}} = 8.95\%$	$R_{\text{bragg}} = 2.44\%$	$\chi^2 = 1.60$	

Atomic position							
Atom	Wyckoff position	x/a	y/b	z/c	occupancy	Biso	BVS
Li1	$4f$	0.1732(11)	0.0002(10)	0.1743(14)	0.702(13)	1.01(11)	1.072(10)
Li2	$2e$	0.622(3)	1/4	0.300(3)	0.50(2)	2.3(4)	0.891(14)
Li3	$2e$	0.814(2)	1/4	0.358(2)	0.52(2)	0.7(2)	0.966(11)
Li4	$4f$	0.383(3)	0.032(3)	0.151(3)	0.285(14)	1.2(3)	0.99(3)
Li5	$4f$	0.059(4)	0.542(3)	0.446(4)	0.189(11)	0.0(3)	0.97(3)
Li6	$2e$	0.972(6)	1/4	0.031(5)	0.240(18)	1.8(6)	0.702(18)
Si/P	$2e$	0.3303(4)	1/4	0.6734(5)	0.75/0.25	0.47*	4.135/4.058(15)
O1	$4f$	0.2236(3)	0.03355(19)	0.8142(3)	1	0.79*	1.899(9)
O2	$2e$	0.6478(4)	1/4	0.6842(4)	1	0.87*	1.888(12)
O3	$2e$	0.2309(4)	1/4	0.3872(4)	1	0.79*	1.986(12)

*Anisotropic thermal parameters (Å^2) x 10^{-4}						
	B11	B22	B33	B12	B13	B23
Si/P	67(10)	27(6)	37(10)	0	-3(7)	0
O1	90(5)	48(3)	62(6)	21(4)	11(4)	-19(3)
O2	89(7)	31(5)	112(8)	0	-14(6)	0
O3	142(8)	26(5)	35(7)	0	-37(6)	0

Si/PO₄	O1^{a**}	O1^b	O2	O3
O1 ^a	<i>1.6150(19)</i>	110.00(14)	108.89(18)	109.43(19)
O1 ^b	2.6459(16)	<i>1.6150(19)</i>	108.89(18)	109.43(19)
O2	2.633(2)	2.633(2)	<i>1.622(3)</i>	110.2(2)
O3	2.621(2)	2.621(2)	2.639(3)	<i>1.595(3)</i>

**O1^a (x,y,z), O1^b (x, 1/2-y, z)

Table S5 (continue)

Li(1)O₄	O1 ^a	O1 ^b	O2	O3
O1 ^a	1.937(8)	100.3(3)	113.6(3)	118.3(3)
O1 ^b	3.052(2)	2.038(6)	112.1(3)	102.2(3)
O2	3.236(2)	3.292(2)	1.930(6)	109.4(3)
O3	3.311(2)	3.081(2)	3.1416(7)	1.920(7)

Li(2)O₄	O1 ^a	O1 ^b	O2	O3
O1 ^a	1.999(8)	120.2(3)	106.2(5)	117.0(5)
O1 ^b	3.4663(16)	1.999(8)	106.2(5)	117.0(5)
O2	3.229(2)	3.229(2)	2.038(16)	80.3(6)
O3	3.455(2)	3.455(2)	2.639(3)	2.052(16)

Li(3)O₄	O1 ^a	O1 ^b	O2	O3
O1 ^a	1.967(5)	123.5(2)	111.9(4)	97.4(3)
O1 ^b	3.4663(16)	1.967(5)	111.9(4)	97.4(3)
O2	3.229(2)	3.229(2)	1.930(11)	112.3(4)
O3	3.081(2)	3.081(2)	3.376(3)	2.133(10)

Li(4)O₄	O1 ^a	O1 ^b	O2	O3
O1 ^a	2.055(16)	118.9(6)	82.4(7)	117.4(7)
O1 ^b	3.455(2)	1.956(16)	112.4(7)	114.1(7)
O2	2.633(2)	3.236(2)	1.939(18)	106.2(7)
O3	3.455(2)	3.311(2)	3.1416(7)	1.989(17)

Li(5)O₅	O1 ^a	O1 ^b	O2	O3 ^a	O3 ^b
O1 ^a	1.99(2)	153.2(8)	107.8(8)	78.6(8)	100.6(8)
O1 ^b	4.045(2)	2.17(2)	98.8(8)	91.2(8)	77.5(8)
O2	3.292(2)	3.229(2)	2.08(2)	105.9(8)	100.1(8)
O3 ^a	2.621(2)	3.081(2)	3.376(3)	2.15(2)	153.0(8)
O3 ^b	3.081(2)	2.621(2)	3.1416(7)	4.0451(19)	2.014(19)

Li(6)O₆	O1 ^a	O1 ^b	O1 ^c	O1 ^d	O2	O3
O1 ^a	2.18(2)	164.1(8)	89.3(8)	74.9(9)	90.1(9)	95.4(9)
O1 ^b	4.2994(19)	2.164(17)	106.4(7)	89.3(8)	88.5(8)	87.3(8)
O1 ^c	3.052(2)	3.4663(16)	2.164(17)	164.1(8)	88.5(8)	87.3(8)
O1 ^d	2.6460(16)	3.052(2)	4.2994(19)	2.18(2)	90.1(9)	95.4(9)
O2	3.292(2)	3.236(2)	3.236(2)	3.292(2)	2.46(3)	172.9(10)
O3	3.311(2)	3.081(2)	3.081(2)	3.311(2)	4.752(3)	2.30(3)

Table S6. Crystallographic data of $\text{Li}_{3.25}\text{Si}_{0.25}\text{P}_{0.75}\text{O}_4$ derived from Rietveld refinements of room temperature powder neutron diffraction patterns and selected interatomic distances (Å) and angles (°). For the Si/PO_4 (or LiO_n) polyhedra the italicized numbers on the diagonal represent the Si/P-O (or Li-O) distances, the numbers above the diagonal are O-Si/P-O (or O-Li-O) angles and the numbers below the diagonal are O-O distances.

$\text{Li}_{3.25}\text{Si}_{0.25}\text{P}_{0.75}\text{O}_4$		
S.G.: $Pnma$;	$Z = 4$	
$a = 10.5259(2)\text{Å}$	$b = 6.1153(2)\text{Å}$	$c = 4.9703(2)\text{Å}$
$V = 319.930(5)\text{Å}^3$	$V/Z = 79.983\text{Å}^3$	$\sum \text{Occ.}(\text{Li}) = 3.24(17) / \text{f.u.}$
$R_{\text{wp}} = 10.7\%$	$R_{\text{bragg}} = 3.70\%$	$\chi^2 = 2.94$

Atomic position							
atom	Wyckoff position	x/a	y/b	z/c	occupancy	Biso	BVS
Li1	8 <i>d</i>	0.1641(5)	0.0007(8)	0.1899(14)	0.86(2)	0.67(16)	1.071(8)
Li2	4 <i>c</i>	0.4266(8)	1/4	0.304(2)	0.90(3)	1.4(2)	0.974(10)
Li3	4 <i>c</i>	0.396(8)	1/4	0.14(2)	0.09(2)	1.5	0.81(8)
Li4	8 <i>d</i>	0.040(6)	0.032(11)	0.075(13)	0.073(10)	1.5	1.12(10)
Li5	8 <i>d</i>	0.147(4)	0.553(6)	0.340(9)	0.16(2)	2.3(10)	1.13(8)
Li6	4 <i>c</i>	0.262(14)	1/4	0.09(2)	0.064(14)	1.5	0.63(8)
Si/P	4 <i>c</i>	0.0884(2)	1/4	0.6813(5)	0.25/0.75	0.47*	4.675/4.588(16)
O1	8 <i>d</i>	0.34140(14)	0.5415(2)	0.2873(3)	1	0.63*	1.917(10)
O2	4 <i>c</i>	0.4473(2)	1/4	0.7151(5)	1	0.79*	2.066(19)
O3	4 <i>c</i>	0.0900(2)	1/4	0.3668(4)	1	0.79*	2.068(15)

Anisotropic thermal parameters (Å^2) $\times 10^{-4}$						
	B11	B22	B33	B12	B13	B23
Si/P	14(3)	30(7)	35(11)	0	0(5)	0
O1	12(2)	44(4)	70(7)	-12(2)	6(3)	-18(5)
O2	14(3)	33(6)	128(12)	0	-9(4)	0
O3	29(3)	34(6)	58(11)	0	-7(4)	0

Si/PO ₄	O1 ^{a**}	O1 ^b	O2	O3
O1 ^a	<i>1.5652(18)</i>	109.10(14)	109.61(19)	109.38(19)
O1 ^b	2.5501(17)	<i>1.5652(18)</i>	109.61(19)	109.38(19)
O2	2.564(2)	2.564(2)	<i>1.572(3)</i>	109.8(2)
O3	2.552(2)	2.552(2)	2.564(3)	<i>1.563(3)</i>

**O1^a (x,y,z), O1^b (x, 1/2-y, z)

Table S6 (continue)

Li(1)O₄	O1 ^a	O1 ^b	O2	O3
O1 ^a	2.017(7)	106.9(3)	98.3(3)	110.1(3)
O1 ^b	3.184(2)	1.945(6)	117.4(3)	112.3(3)
O2	2.990(2)	3.315(2)	1.934(5)	110.6(2)
O3	3.232(2)	3.215(2)	3.1736(8)	1.925(6)

Li(2)O₄	O1 ^a	O1 ^b	O2	O3
O1 ^a	1.997(4)	126.39(19)	95.1(3)	112.6(3)
O1 ^b	3.5652(17)	1.997(4)	95.1(3)	112.6(3)
O2	2.990(2)	2.990(2)	2.055(10)	110.2(4)
O3	3.258(2)	3.258(2)	3.259(3)	1.918(9)

Li(3)O₄	O1 ^a	O1 ^b	O2	O3
O1 ^a	2.01(4)	124.9(18)	115(3)	107(3)
O1 ^b	3.5652(17)	2.01(4)	115(3)	107(3)
O2	3.537(3)	3.537(3)	2.18(10)	75(4)
O3	3.258(2)	3.258(2)	2.564(3)	2.04(8)

Li(4)O₅	O1 ^a	O1 ^b	O2 ^a	O2 ^b	O3
O1 ^a	2.25(6)	148(3)	85(2)	77(3)	99(3)
O1 ^b	3.984(2)	1.90(7)	77(3)	105(3)	110(3)
O2 ^a	2.990(2)	2.564(2)	2.19(7)	147(3)	101(3)
O2 ^b	2.564(2)	2.990(2)	3.893(2)	1.86(7)	109(3)
O3	3.258(2)	3.232(2)	3.259(3)	3.1736(8)	2.04(7)

Li(5)O₄	O1 ^a	O1 ^b	O2	O3
O1 ^a	2.06(4)	93.5(16)	124.3(18)	106.3(16)
O1 ^b	3.184(2)	2.30(4)	124.7(18)	73.3(16)
O2	3.315(2)	3.537(3)	1.68(4)	121.6(17)
O3	3.215(2)	2.553(2)	3.1736(8)	1.95(4)

Li(6)O₅	O1 ^a	O1 ^b	O1 ^c	O1 ^d	O3
O1 ^a	2.25(10)	91(3)	160(3)	69(4)	91(4)
O1 ^b	3.184(2)	2.20(7)	108(3)	160(3)	92(4)
O1 ^c	4.3849(19)	3.5652(17)	2.20(7)	91(3)	92(4)
O1 ^d	2.5501(17)	4.3849(19)	3.184(2)	2.25(10)	91(4)
O3	3.232(2)	3.215(2)	3.215(2)	3.232(2)	2.27(13)

Table S7. Average Si/P-O bond lengths for (1-z) Li₄SiO₄ - z Li₃PO₄ obtained from Rietveld refinements and linear interpolation between Li₄SiO₄ and Li₃PO₄ (Å)

Si/P-O distance (Å)	Li ₄ SiO ₄	z=0.25	z=0.5	z=0.75	Li ₃ PO ₄
Rietveld refinement	1.641	1.612	1.587	1.566	1.544
Linear interpolation	1.641	1.617	1.592	1.568	1.544

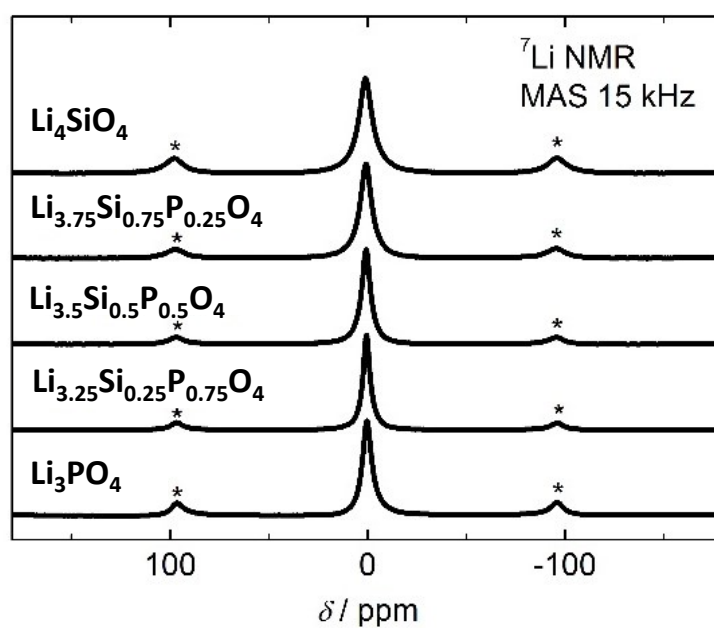


Figure S8. ⁷Li MAS (15 kHz) NMR signals at ambient temperature. Rotational sidebands are marked with an asterisk.

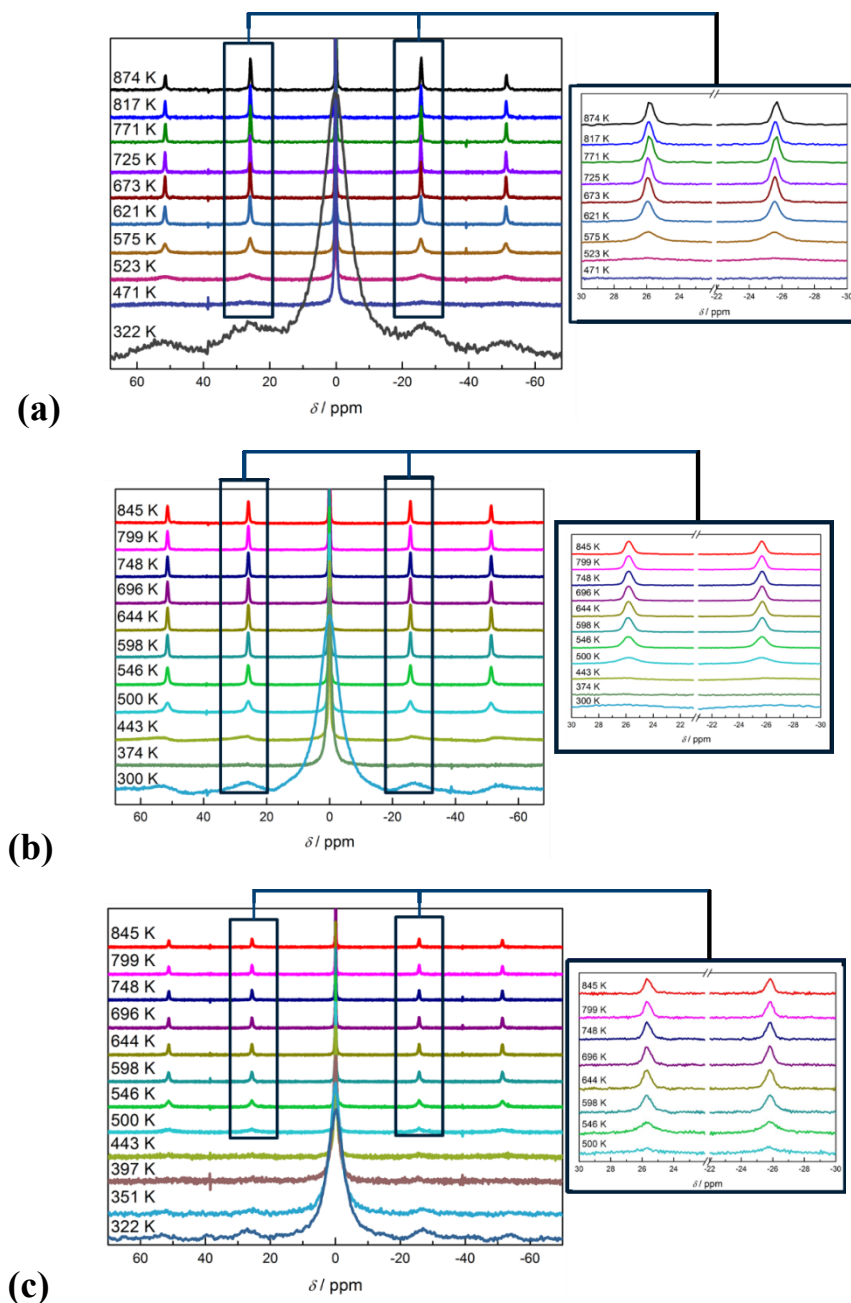


Figure S9. Temperature dependent ${}^7\text{Li}$ NMR signal line shape development in a magnetic field of 9.4 T and a MAS rate of 4 kHz. Full spectra (left) and a zoom of the rotational sidebands (right) are shown, for (a) $\text{Li}_{3.75}\text{Si}_{0.75}\text{P}_{0.25}\text{O}_4$, (b) $\text{Li}_{3.5}\text{Si}_{0.5}\text{P}_{0.5}\text{O}_4$ and (c) $\text{Li}_{3.25}\text{Si}_{0.25}\text{P}_{0.75}\text{O}_4$

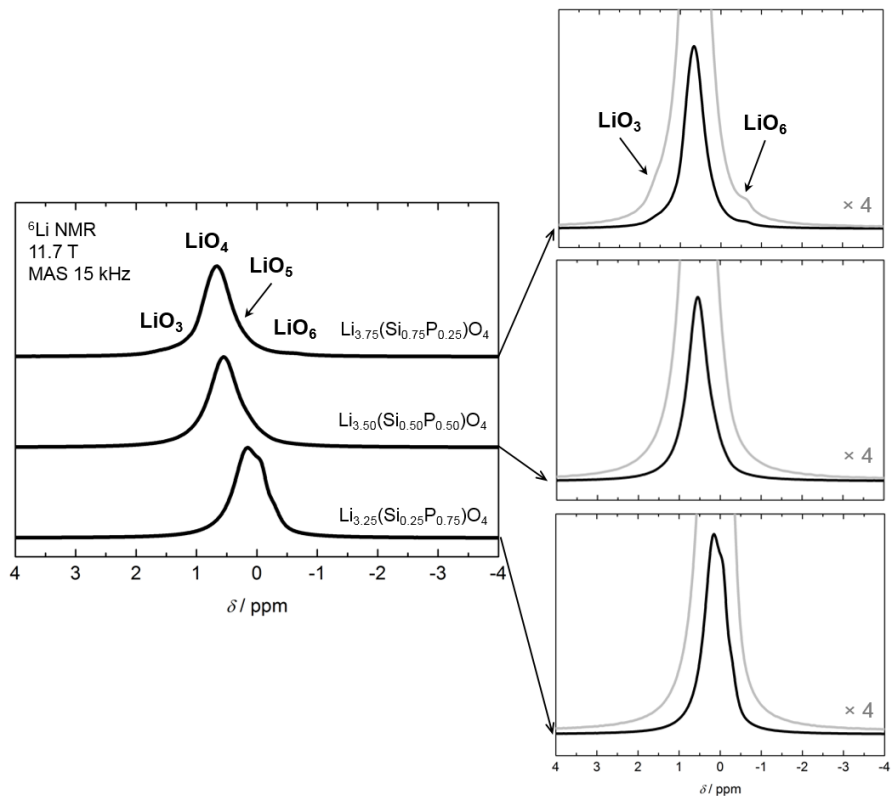


Figure S10. ⁶Li MAS NMR of Li_{3.75}Si_{0.75}P_{0.25}O₄, Li_{3.5}Si_{0.50}P_{0.50}O₄, and Li_{3.25}Si_{0.25}P_{0.75}O₄ at 15 kHz MAS speed in a magnetic field of 11.7 T at 298 K. The right figures show the spectra separately with the normalized intensity (black lines) and 4times up scaled intensity (grey lines).

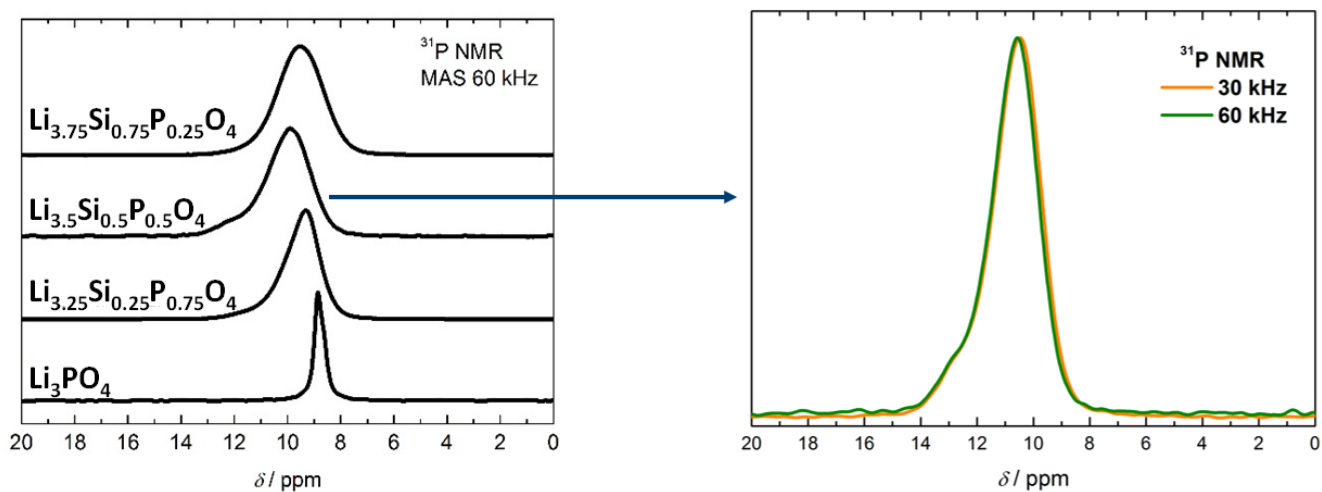


Figure S11. ³¹P MAS (60 kHz) NMR spectra of the pure phosphate and solid solution samples at ambient temperature. Only the isotropic line is shown. The right picture shows the comparison of the NMR signal line shape of Li_{3.5}Si_{0.5}P_{0.5}O₄ at MAS spinning speeds of 60 and 30 kHz.

Table S12. Comparison of the calculated and experimental structural parameters of $\text{Li}_{3.75}\text{Si}_{0.75}\text{P}_{0.25}\text{O}_4$ and $\text{Li}_{3.25}\text{Si}_{0.25}\text{P}_{0.75}\text{O}_4$

$\text{Li}_{3.75}\text{Si}_{0.75}\text{P}_{0.25}\text{O}_4$	a (Å)	b (Å)	c (Å)	β (°)	$M-O$ (Å)	$Li-O$ (Å)
Expt.	5.105	6.112	5.297	90.37	1.612	2.110
Calc.	5.248	6.065	5.255	88.03	1.584	2.064
Δ	0.143	-0.047	-0.042	-2.34	-0.028	-0.046

$\text{Li}_{3.25}\text{Si}_{0.25}\text{P}_{0.75}\text{O}_4$	a (Å)	b (Å)	c (Å)	$M-O$ (Å)	$Li-O$ (Å)
Expt.	10.526	6.115	4.970	1.566	2.080
Calc.	10.636	6.151	5.054	1.542	2.073
Δ	0.110	0.036	0.084	-0.024	-0.007

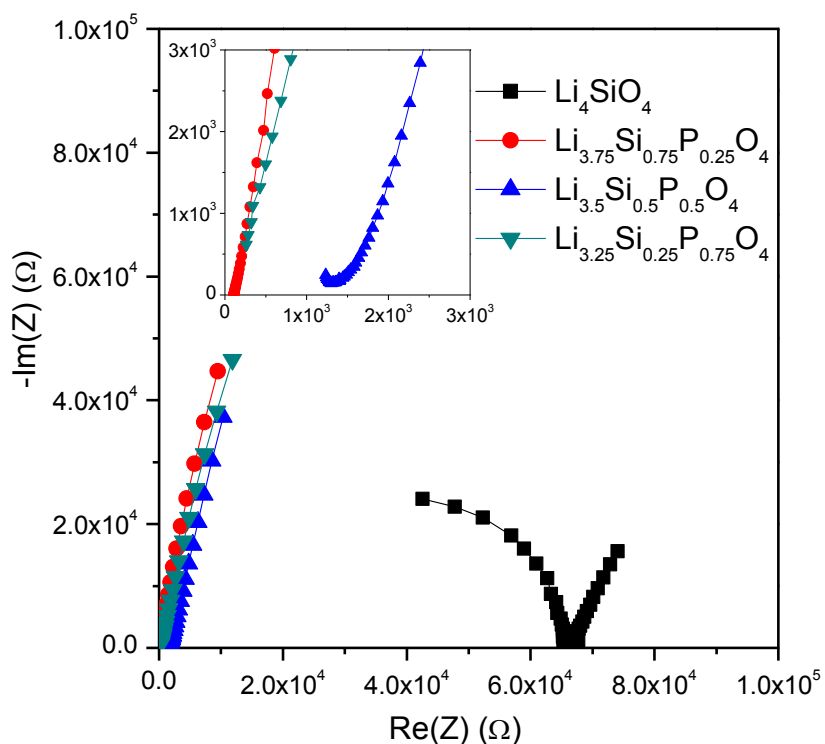


Figure S13. AC impedance spectra of Li_4SiO_4 , $\text{Li}_{3.75}\text{Si}_{0.75}\text{P}_{0.25}\text{O}_4$, $\text{Li}_{3.5}\text{Si}_{0.5}\text{P}_{0.5}\text{O}_4$ and $\text{Li}_{3.25}\text{Si}_{0.25}\text{P}_{0.75}\text{O}_4$ measured at 573K. Inserted: low resistance region showing high frequency details for the solid solution compositions.

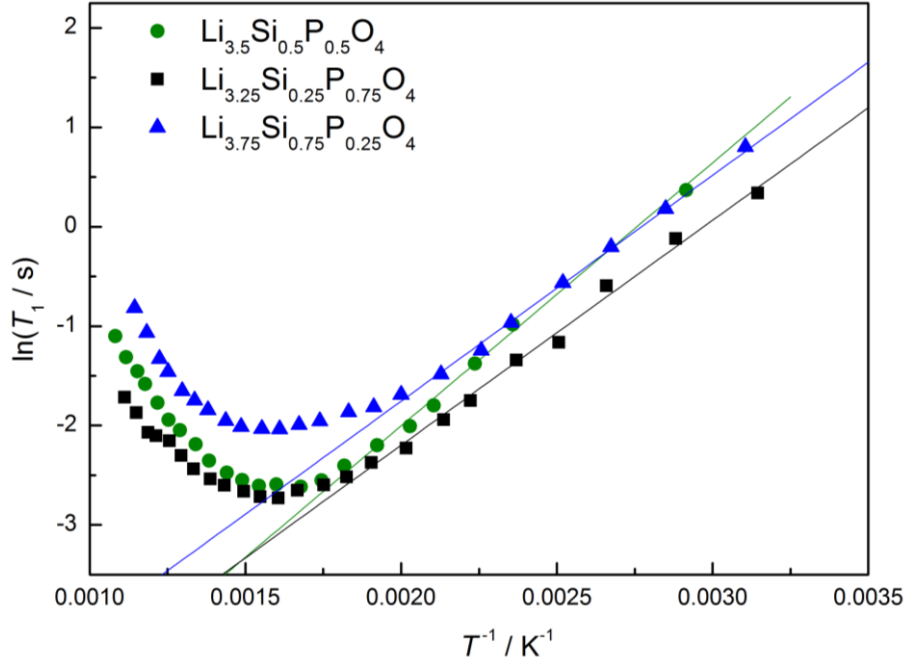


Figure S14. Arrhenius plot of ${}^7\text{Li}$ T_1 values. Linear fitting are used at low temperature regimes to determine the respective E_{act} (straight lines).

Table S15. Comparison of the activation energies derived from ${}^7\text{Li}$ T_1 data fits based on an Arrhenius plot analysis vs. BPP fits. Single standard deviations are given in parenthesis. Furthermore, the activation energies based on the MD modeling and AC impedance spectroscopy (EIS) measurements are given.

B_0 / T	9.4	9.4	MD modeling	EIS
T / K	320 – 875	320 – 875	473 – 673	323 – 573
Fit method	Arrhenius	BPP	Arrhenius	Arrhenius
Sample	E_a / eV			
$\text{Li}_{3.75}\text{Si}_{0.75}\text{P}_{0.25}\text{O}_4$	0.19(1)	0.18(3)	0.31	0.48
$\text{Li}_{3.5}\text{Si}_{0.5}\text{P}_{0.5}\text{O}_4$	0.22(1)	0.23(2)	0.32	0.49
$\text{Li}_{3.25}\text{Si}_{0.25}\text{P}_{0.75}\text{O}_4$	0.20(1)	0.21(2)	0.30	0.44

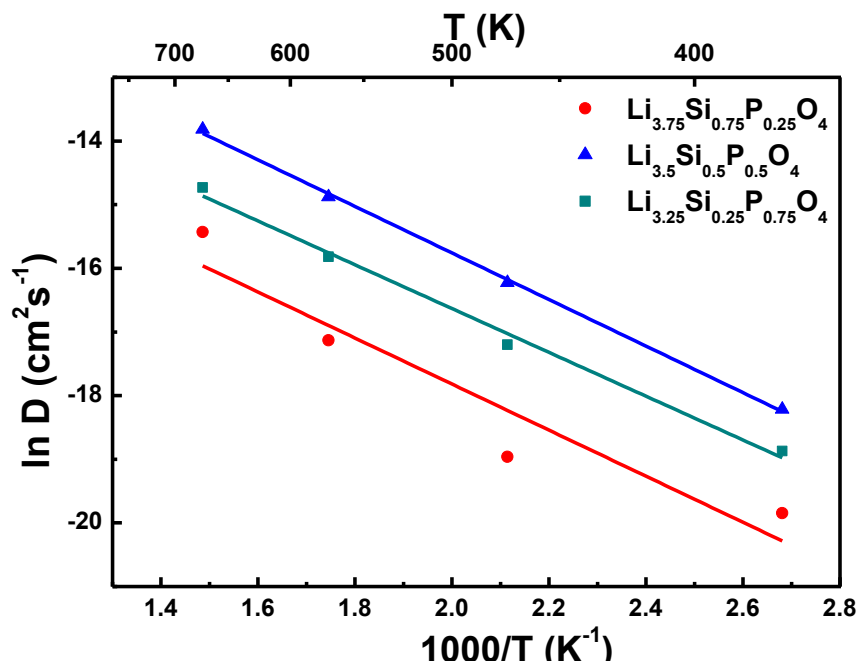


Figure S16. Arrhenius plots ($\ln D_{Li}$ versus $1/T$) for $\text{Li}_{3.75}\text{Si}_{0.75}\text{P}_{0.25}\text{O}_4$ (red circles), $\text{Li}_{3.5}\text{Si}_{0.5}\text{P}_{0.5}\text{O}_4$ (blue triangles) and $\text{Li}_{3.25}\text{Si}_{0.25}\text{P}_{0.75}\text{O}_4$ (cyan squares) from MD modeling.

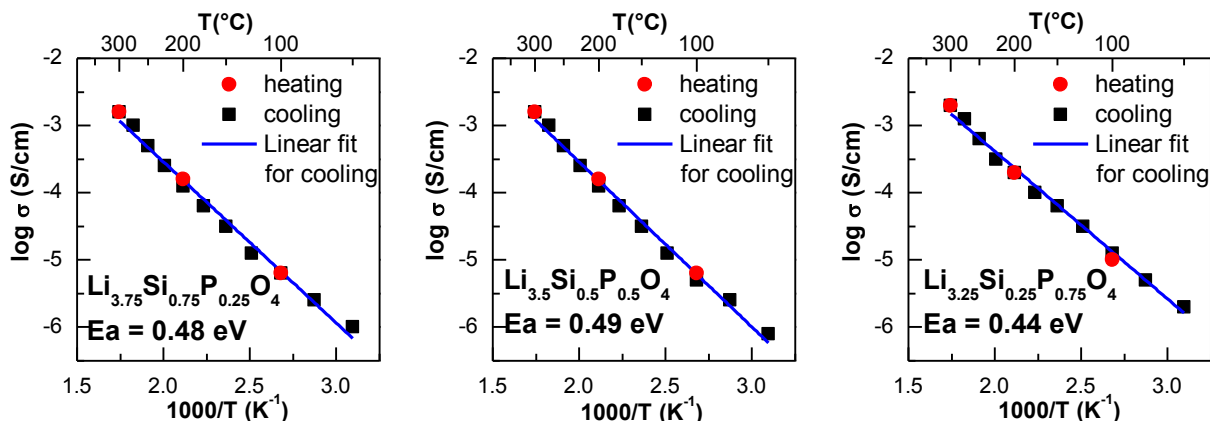


Figure S17. Arrhenius plots for (from left to right) $\text{Li}_{3.75}\text{Si}_{0.75}\text{P}_{0.25}\text{O}_4$, $\text{Li}_{3.5}\text{Si}_{0.5}\text{P}_{0.5}\text{O}_4$ and $\text{Li}_{3.25}\text{Si}_{0.25}\text{P}_{0.75}\text{O}_4$ from AC impedance measurements. For each sample, data was recorded at 100, 200 and 300°C during heating (red circles) and every 25°C during cooling from 300°C to 50°C (black squares). Activation energies deriving from linear fit of data from cooling process (blue line) are shown in text.

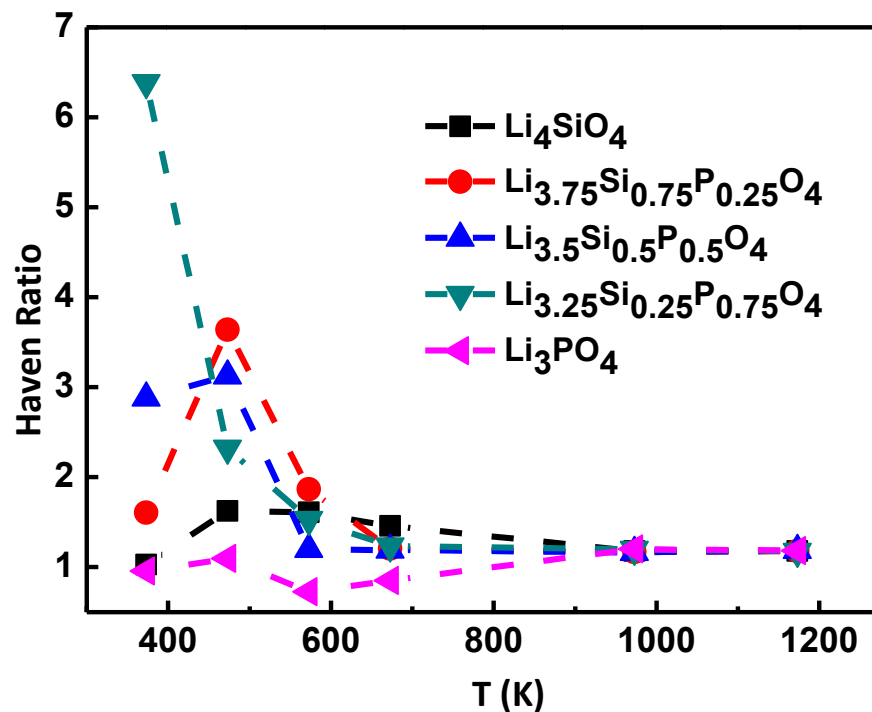


Figure S18. Calculated Haven ratio values versus temperature for Li_4SiO_4 , $\text{Li}_{3.75}\text{Si}_{0.75}\text{P}_{0.25}\text{O}_4$, $\text{Li}_{3.5}\text{Si}_{0.5}\text{P}_{0.5}\text{O}_4$, $\text{Li}_{3.25}\text{Si}_{0.25}\text{P}_{0.75}\text{O}_4$ and Li_3PO_4 . The Haven ratio is defined as the ratio of the tracer diffusion coefficient to the chemical diffusion coefficient. Values > 1.0 indicate cooperative diffusion whereas values equal to 1.0 indicate uncorrelated Li ion motion. Some values for Li_3PO_4 are slightly less than one due to its very low conductivity and poorer statistics.